



### **Geophysical Research Letters**\*



#### RESEARCH LETTER

10.1029/2025GL117351

Kai Huang, Wenbin Ling, and Huibo Tang contributed equally to this work.

#### **Key Points:**

- Magnetic reconnection in a magnetopause-like geometry is experimentally studied in Space Plasma Environment Research Facility
- Bipolar and Quadrupole Hall magnetic fields confirm that reconnection is in Hall regime
- Reconnection evolves from asymmetric multiple x-line state to symmetric single x-line state

#### Correspondence to:

P. E and Q. Lu, epeng@hit.edu.cn; qmlu@ustc.edu.cn

#### Citation:

Huang, K., Ling, W., Tang, H., Guan, J., Yang, J., Xie, J., et al. (2025). Laboratory realization of magnetopause-like reconnection in Space Plasma Environment Research Facility (SPERF). *Geophysical Research Letters*, 52, e2025GL117351. https://doi.org/10.1029/ 2025GL117351

Received 1 JUN 2025 Accepted 28 SEP 2025

# © 2025. The Author(s). This is an open access article under the terms of the Creative Commons Attribution License, which permits use, distribution and reproduction in any medium, provided the original work is properly cited.

## Laboratory Realization of Magnetopause-Like Reconnection in Space Plasma Environment Research Facility (SPERF)

Kai Huang<sup>1</sup> , Wenbin Ling<sup>2</sup>, Huibo Tang<sup>1</sup> , Jian Guan<sup>2</sup>, Jihua Yang<sup>3</sup>, Jiayin Xie<sup>4</sup>, Gaoyuan Peng<sup>4</sup>, Hanru Ma<sup>1</sup>, Nan Wang<sup>1</sup>, Tianyi Zhang<sup>1</sup> , Zheng Cao<sup>3</sup>, Shangkun Ren<sup>4</sup>, Yangguang Ke<sup>4</sup> , Ke Han<sup>5</sup>, Yunning Dong<sup>6</sup>, Yaowen Lu<sup>6</sup>, Peng E<sup>2,4</sup> , and Quanming Lu<sup>7,8,9</sup>

<sup>1</sup>School of Physics, Harbin Institute of Technology, Harbin, China, <sup>2</sup>State Key Laboratory of Space Environment Interaction with Matters, Harbin Institute of Technology, Harbin, China, <sup>3</sup>School of Electrical Engineering and Automation, Harbin Institute of Technology, Harbin, China, <sup>4</sup>School of Energy Science and Engineering, Harbin Institute of Technology, Harbin, China, <sup>5</sup>School of Computer and Information Engineering, Harbin University of Commerce, Harbin, China, <sup>6</sup>Beijing Orient Institute of Measurement & Test, Beijing, China, <sup>7</sup>Deep Space Exploration Laboratory, School of Earth and Space Sciences, University of Science and Technology of China, Hefei, China, <sup>8</sup>CAS Center for Excellence in Comparative Planetology, CAS Key Lab of Geospace Environment, University of Science and Technology of China, Hefei, China, <sup>9</sup>Collaborative Innovation Center of Astronautical Science and Technology, Harbin, China

**Abstract** Magnetic reconnection explosively converts magnetic energy into plasma heating and particle acceleration. At Earth's magnetopause, reconnection governs solar wind-magnetosphere coupling and drives global convection. Understanding these processes requires resolving reconnection's spatiotemporal evolution, which is difficult for in situ observations but achievable in laboratory experiments. However, building a geometry like the real magnetopause in laboratory remains a key challenge. Here, we present the first laboratory experiment at the Space Plasma Environment Research Facility trying to replicates Earth's magnetopause configuration. Using a dipole magnet (mimicking magnetosphere) and coaxial flux cores (simulating solar wind), we establish a magnetopause-like current sheet via dynamic plasma compression. Measured Hall magnetic fields confirm Hall reconnection, transitioning from an asymmetric multiple x-lines state to a symmetric single x-line state. This dynamic evolution will impact global energy conversion and transport at magnetopause.

Plain Language Summary The interaction between solar wind and Earth's magnetosphere forms a boundary layer named magnetopause, where a fundamental plasma process, magnetic reconnection, usually takes place. During magnetopause reconnection, a huge amount of energy can be released, leading to explosive geomagnetic activities. Although magnetopause reconnection has been extensively studied by satellite observations, its spatial and temporal evolution have not been well understood because of the limited spacecraft trajectories. Here, taking advantage of the repeatability and controllability of laboratory plasma experiment, we try to experimentally study magnetopause reconnection by building a magnetopause-like geometry in a new device: Space Plasma Environment Research Facility. The results show dynamic evolution of reconnection with features similar to previous observations and simulations. We believe this platform will greatly advance studies of the interaction between solar wind and planetary magnetosphere.

#### 1. Introduction

Magnetic reconnection, a universal plasma process that explosively converts magnetic energy into plasma heating and particle acceleration, powers some of the most energetic phenomena in the universe, from solar flares and magnetospheric substorms to gamma ray bursts (Angelopoulos et al., 2008, 2020; Kumar & Zhang, 2015; Lu et al., 2022; Lyutikov & Lazarian, 2013; Masuda et al., 1994; Shibata et al., 1995). For planets with intrinsic magnetic field like Earth, the interaction between their magnetosphere with solar wind forms a boundary layer named magnetopause (DiBraccio et al., 2013; Frey et al., 2003; Huddleston et al., 1997; McAndrews et al., 2008; Paschmann et al., 1979; Phan et al., 2000; Slavin et al., 2009; Sonnerup et al., 1981; Walker & Russell, 2012). Magnetic reconnection is one of the most important processes take place at magnetopause because it mediates the transfer of solar wind energy into the magnetosphere, driving global convection and substorms (Burch et al., 2016; Dai et al., 2024; Dungey, 1961). Magnetopause reconnection usually occurs under strong solar wind compression and significant plasma asymmetries, leading to dynamic evolution of reconnection region with complex structures. Satellite missions (e.g., Cluster, THEMIS, MMS) have identified some key reconnection

features such as the Hall magnetic and electric fields (Mozer et al., 2002; Tanaka et al., 2008; Vaivads et al., 2004; R. Wang, Nakamura, et al., 2017), the formation and interaction of magnetic flux ropes (Øieroset et al., 2011; Sonnerup et al., 2004; R. Wang, Lu, et al., 2017; Zhou et al., 2017). However, these observations are inherently limited to measurements along spacecraft trajectories, the time-dependent and global evolution of magnetopause reconnection, which are important for the energy conversion and transport processes, remains incompletely understood.

Laboratory experiments have emerged as critical tools to resolve these spatiotemporal gaps (Ji et al., 2023). Facilities such as VTF (Egedal et al., 2003), MRX (Ji et al., 1998; Yamada et al., 2014, 2018), TREX (Greess et al., 2021; Olson et al., 2016), PHASMA (Shi et al., 2022, 2023), and KLMP (Sang et al., 2022; F. Yang et al., 2025) have made great progresses in understanding fundamental problems in reconnection through delicate experiment design and precise diagnostics, yet replicating the magnetopause's geometry and driven conditions has remained a frontier challenge. To address this, the Space Plasma Environment Research Facility (SPERF) was developed, which is a large-scale cylindrical device with a length of 10.5 m and a diameter of 5 m. SPERF uniquely integrates a dipole magnet (emulating Earth's dipole field) with four pulsed coaxial flux cores (simulating solar wind magnetic fields). This configuration compresses a high-speed plasma against the dipole field, self-consistently forming a magnetopause-like current sheet with parameters directly scalable to space conditions (Ling et al., 2022, 2024).

In this work, we employ SPERF to experimentally study magnetopause reconnection. High-resolution measurements detect Hall magnetic field consistent with spacecraft observations, indicating the process of Hall reconnection. The reconnection current sheet has a two-stage evolution: an initial asymmetric phase, marked by multiple reconnection *x*-lines and magnetic island formation, transitions to a symmetric single *x*-line regime. Although the spatial scale and Lundquist number of the current experiment remain far different from Earth's magnetopause, our results provide valuable interpretation for the dynamic evolution of magnetopause-like reconnection, demonstrating the capability of SPERF to establish a scalable platform for studying space plasma physics in laboratory.

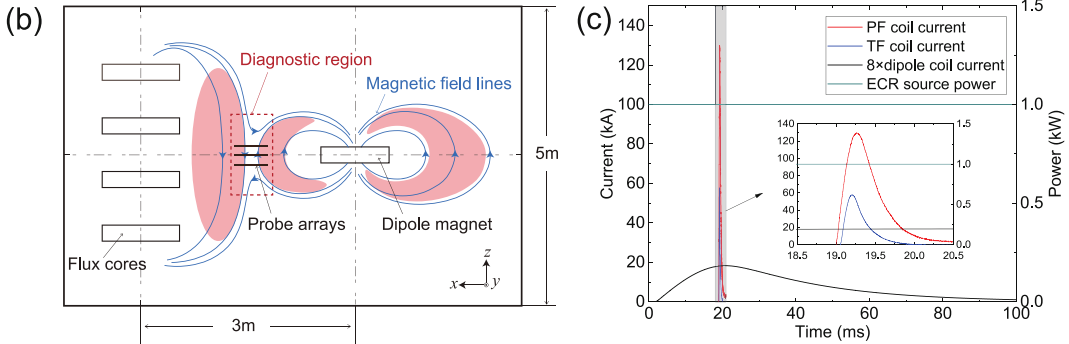
#### 2. Experimental Setup

Figure 1a shows a schematic of SPERF. The experiment setup is as follows. An electron cyclotron resonant (ECR) plasma source is triggered first to inject microwave into the apparatus constantly. Then, data acquisition for the magnetic field begins at time 0, and a slow pulsed current is driven in the dipole magnet at 2 ms to create a dipole magnetic field. A quasi-steady model magnetosphere is built when the current peaks at 19 ms, at the same time, the poloidal field (PF) coils of the four flux cores are driven by rapid pulsed currents to create the model solar wind magnetic field. After a delay of 50  $\mu$ s, the model solar wind plasma is inductively generated around the flux cores by their toroidal field coils driven by rapid pulsed currents. The simulated solar wind expands outwards and compresses the model magnetosphere, inducing magnetic reconnection, as shown in Figure 1b. The time sequence of the experiment is detailed in Figure 1c. In the following of this paper, we will omit "model" before "magnetosphere" and "solar wind" for simplification. Argon is used as the discharging gas, and the fill pressure is set as 0.5 Pa. Some typical plasma parameters are summarized in Table 1.

We use a coordinate system similar to the GSM coordinate system: The origin point is located at the center of the dipole magnet, x-axis points to the four flux cores horizontally, z-axis points upward vertically, and y-axis completes the right-hand system (see Figure 1b). A movable 3D magnetic probe array is adopted to measure the three components of the magnetic field at  $16 \times 21$  locations spanning a region of  $32 \times 84$  cm centered at x = 150 cm and z = 0 in the y = 0 plane (J. Yang et al., 2024). The magnetic probe array is made of miniature commercial inductive coils, whose areas have good uniformity. They are calibrated by a Helmholtz coil. The magnetic field measurement errors are smaller than 10%. The response frequency of the magnetic probes is better than 300 kHz, and their spatial resolution is about 5 mm. The Langmuir probes with four tips are used for plasma density and electron temperature measurements. Their temporal and spatial resolutions are better than 0.5  $\mu$ s and 10 mm. The errors of the electrostatic measurement are lower than 50%.

HUANG ET AL. 2 of 9

19448007, 2025, 20, Downloaded from https://agupubs.onlinelibrary.wiley.com/doi/10.1029/2025GL117351 by University Of Science, Wiley Online Library on [17/10/2025]. See the Terms and Conditions (https://doi.org/10.1029/20256117351).



**Figure 1.** (a) A schematic of Space Plasma Environment Research Facility (SPERF). (b) A sketch of the magnetopause reconnection experiment in SPERF and our diagnostic region. (c) The time sequence of the experiment.

#### 3. Experimental Results

#### 3.1. Spatial Distribution of Magnetic Field

Figure 2 shows the spatial distribution of the three components of magnetic field at t=19.135 ms, during the growth phase of the driving current in the flux cores. In Figure 2a,  $B_x$  shows clear bipolar structure corresponding to a magnetic island, which is bounded by two reconnection x-lines. On the solar wind side, the amplitude of  $B_z$  can reach 200 Gs, while on the magnetosphere side, it is only around 100 Gs. The electron density on the solar wind side (around  $10^{13}$  cm<sup>-3</sup>) is also an order of magnitude higher than that on the magnetosphere side (around  $10^{12}$  cm<sup>-3</sup>). Therefore, reconnection is asymmetric during this period. However, the magnetic field asymmetry is a little different from Earth's magnetopause, where it is stronger on the magnetosphere side. The reason might be that the driving current in the flux cores is too large compared with that in the dipole magnet. In Figure 2b, we notice that  $B_y$  shows a bipolar distribution around both x-lines, where it is negative above the x-line and is positive below the x-line. In Figures 2d and 2e, we plot the line profiles of  $B_z$  and  $B_y$  along the two horizontal dashed lines in Figures 2b and 2c, crossing the bipolar  $B_y$  patterns below the top x-line and above the bottom x-line,

**Table 1**Typical Parameters for the Magnetopause Reconnection Experiment in Space Plasma Environment Research Facility

Parameters	Solar wind value	Magnetosphere value
Reconnecting magnetic field B	100-200 Gs	50-100 Gs
Plasma size $L$	1 m	1 m
Electron density $n_e$	$(1-2) \times 10^{13} \text{ cm}^{-3}$	$(0.5-2) \times 10^{12} \text{ cm}^{-3}$
Electron temperature $T_e$	5–20 eV	5–10 eV
Lundquist number S	80-1,800	130-1,500
Mean free path l	1.8–57.6 cm	18-288 cm

respectively. The positive  $B_y$  located around  $B_z = 0$  in Figure 2d is clear. In Figure 2e, there is a negative background  $B_y$ , we can still identify a negative peak of  $B_y$  around  $B_z = 0$ . The polarization of the bipolar  $B_y$  structure also agrees with the Hall magnetic field during asymmetric reconnection, where it is formed due to the Hall current carried mainly by electrons penetrate the magnetosphere from the solar wind (Pritchett, 2008; Shay et al., 2016).

In this period, the typical magnetic field is B=200 Gs, electron density is  $n_e=2\times 10^{13}$  cm<sup>-3</sup>, electron temperature is  $T_e=20$  eV. Then, the Lundquist number is around S=1,300, and the system size normalized by ion inertia length is around  $\lambda=Lld_i=3.1$ . The system is in single x-line collisionless regime based on the phase diagram of reconnection (Ji & Daughton, 2011). However, multiple x-line reconnection with magnetic island still develops, similar result was also obtained in previous works (Stenzel &

HUANG ET AL. 3 of 9

19448007, 2025, 20, Downloaded from https://agupubs.onlinelibrary.wiley.com/doi/10.1029/2025GL117351 by University Of Science, Wiley Online Library on [17/10/2025]. See the Term

and-conditions) on Wiley Online Library for rules of use; OA articles are governed by the applicable Creative Commons License

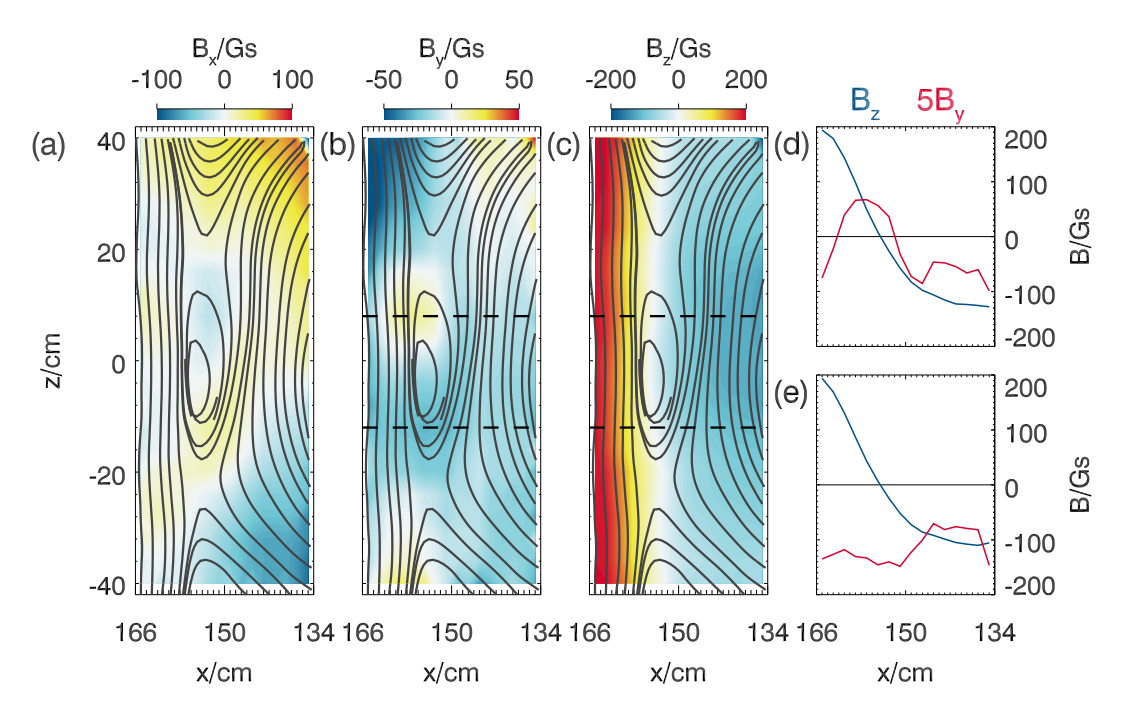


Figure 2. (a–c) The spatial distribution of the three components of magnetic field at t = 19.135 ms, the black curves represent the in-plane magnetic field lines. (d, e) The line profiles of  $B_z$  and  $B_y$  along the two horizontal dashed lines in panels (b, c).

Gekelman, 1981; Xie et al., 2024; Yamada et al., 1997). For our experiment, the formation of the two *x*-lines is related to the non-uniform drive from the four flux cores.

Figure 3 shows the spatial distribution of the three components of magnetic field at t = 19.37 ms, during the early decay phase of the driving current. The distributions of  $B_x$  and  $B_z$  show a typical single x-line geometry.  $B_y$  shows a quadrupole distribution, and the polarization is consistent with the Hall magnetic field. In Figures 3d and 3e, the

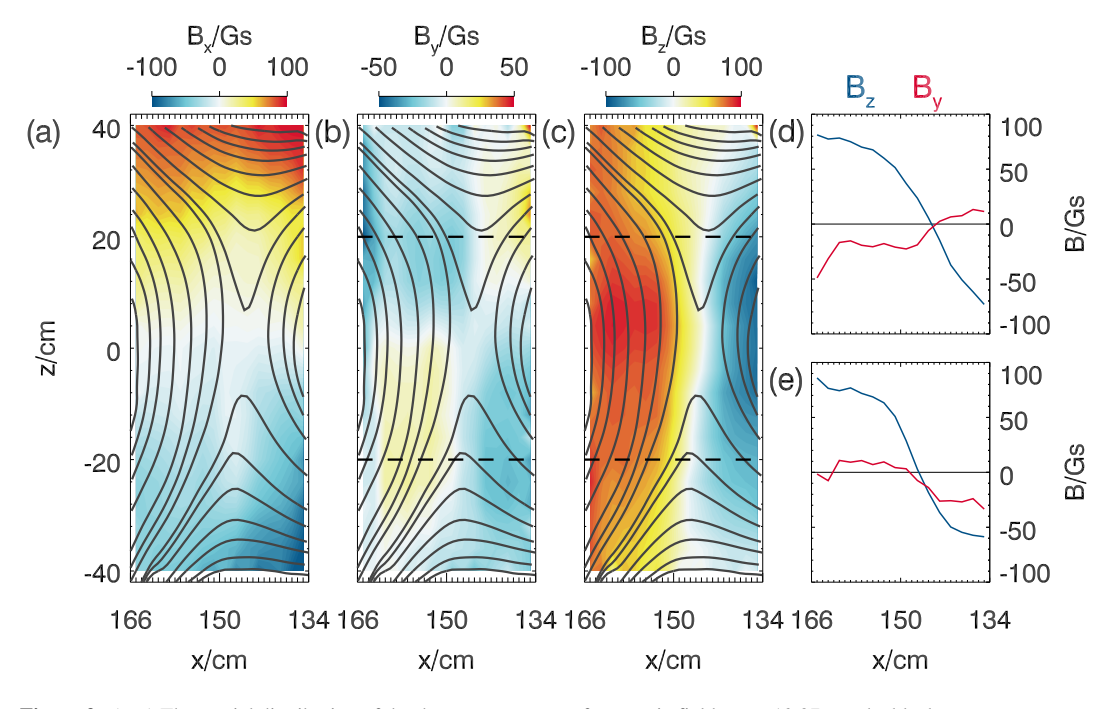


Figure 3. (a–c) The spatial distribution of the three components of magnetic field at t = 19.37 ms, the black curves represent the in-plane magnetic field lines. (d, e) The line profiles of  $B_z$  and  $B_v$  along the two horizontal dashed lines in panels (b, c).

HUANG ET AL. 4 of 9

from https://agupubs.onlinelibrary.wiley.com/doi/10.1029/2025GL117351 by University Of Science, Wiley Online Library on [17/10/2025]

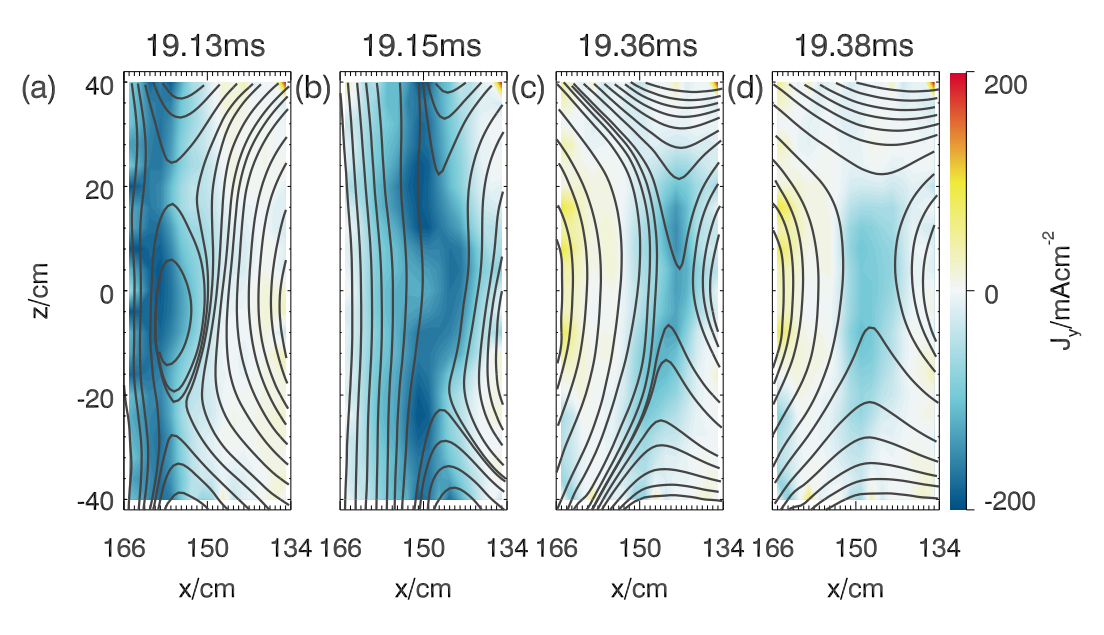


Figure 4. The time evolution of the reconnection current sheet at t = 19.13, 19.15, 19.36, and 19.38 ms. The current density is calculated by  $J_y = (\partial_z B_x - \partial_x B_z)/\mu_0$  using the measured magnetic field  $B_x$  and  $B_z$ . The black curves represent the in-plane magnetic field lines.

amplitude of the Hall magnetic field  $B_y$  can reach 10%–30% of the upstream magnetic field  $B_z$ , it is also consistent with previous studies (Eastwood et al., 2010). In this period, the typical magnetic field is B=100 Gs, electron density is  $n_e=10^{12}$  cm<sup>-3</sup>, electron temperature is  $T_e=10$  eV. Then, the Lundquist number is around S=1,000, and the system size normalized by ion inertia length is around  $\lambda=Lld_i=0.7$ . The system is also in single x-line collisionless regime.

Besides these two time slices, Hall magnetic field persists for a long time during the experiment, indicating that reconnection in our experiment is in the Hall regime. Distinct distributions of Hall magnetic field at different stages also indicate dynamic evolution of the reconnection current sheet, which will be presented in Section 3.2.

#### 3.2. Time Evolution of the Reconnection Current Sheet

During the growth phase of the driving current in the PF coils, the solar wind expands and greatly compresses the magnetosphere. As a result, the reconnecting current sheet sweeps through our probe arrays from the left side to the right side, and then, the reconnecting current sheet moves back due to the rebound of magnetosphere. The time evolution of the reconnection current sheet is shown in Figure 4. In Figures 4a and 4b, the current sheet moves from left to right, while in Figures 4c and 4d, the current sheet is rebounded from right to left. Here, the current density  $J_y = (\partial_z B_x - \partial_x B_z)/\mu_0$  is calculated using the measured magnetic field  $B_x$  and  $B_z$ . In Figures 4a and 4b, the current density  $J_y$  is stronger, and the current sheet is long in the z direction. The magnetic field lines show multiple x-line geometry with a magnetic island in Figure 4a. This magnetic island has formed before  $t \approx 19.12$  ms, when the current sheet starts to move into our diagnostic region, and it disappears at  $t \approx 19.14$  ms. In Figures 4c and 4d, the current density is a little weaker, and the current sheet is short, strong current density only displays near the x-line.

The motion of the reconnection current sheet can be identified clear in Figure 5a, which shows the time stack of the distribution of  $J_y$  along the x direction. The current sheet can be observed during two time periods, t = 19.12–19.17 ms and t = 19.31–19.38 ms, corresponding to the growth phase and early decay phase of the driving current shown in Figure 5b.

Figures 5c and 5d plot the time evolution of the location and the half width of the current sheet. At each time slice, we fit the  $J_y$  distribution along x using a function with the form of  $f(x) \sim \cosh^{-2}((x-x_0)/\delta)$ , the fitted  $x_0$  and  $\delta$  are chosen to be the location and half width of the current sheet. From Figure 5c, we can estimate the motion speeds of the current sheet during the two periods, which are around -5.6 and 1.7 km/s. This motion agrees well with the prediction from the particle-in-cell simulation of magnetic reconnection experiment in SPERF (Huang

HUANG ET AL. 5 of 9

onlinelibrary.wiley.com/doi/10.1029/2025GL117351 by University Of Science, Wiley Online Library on [17/10/2025]. See the

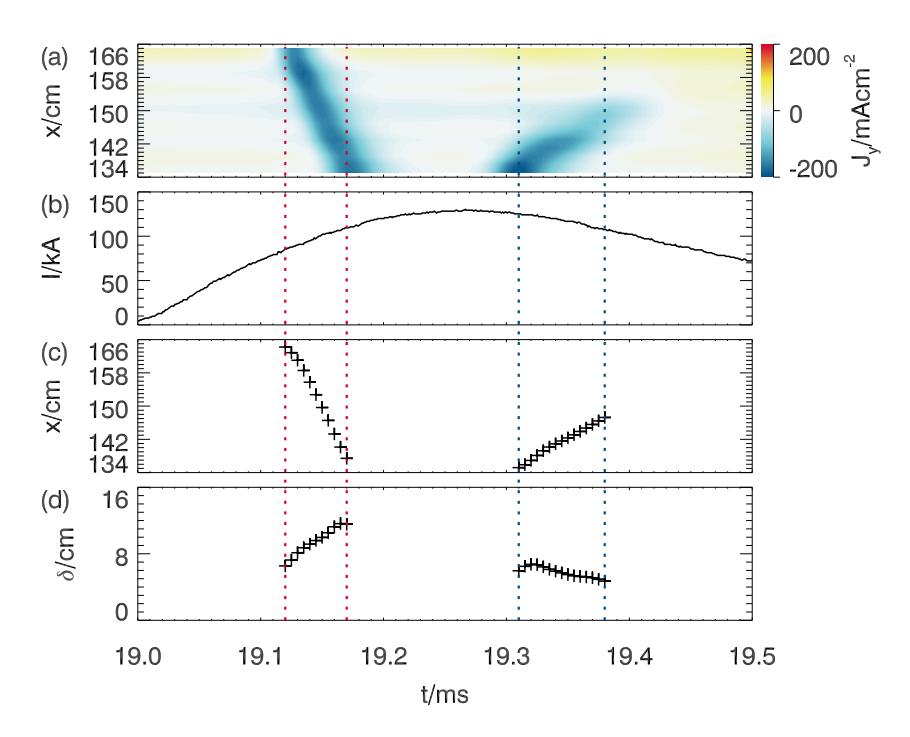


Figure 5. (a) The time stack of the distribution of  $J_y$  along the x direction. (b) The amplitude of the driving current in the poloidal field coils in the flux cores. (c) The time evolution of the location of the reconnection current sheet in the x direction. (d) The half width of the reconnection current sheet. The red and blue dashed lines bound the two time periods during which we measure the current sheet.

et al., 2025). During the first period, the model solar wind magnetic field  $B_z$  is around 200 Gs, and the electron density is around  $n_e \approx 1 \times 10^{13}$  cm<sup>-3</sup>, then the Alfven speed is around  $V_A \approx 21.8$  km/s. So, the normalized motion velocity of the reconnection current sheet is around 0.26  $V_A$ , which can be regarded as the expanding speed of the solar wind. This driving speed is sub-Alfvenic, but a little larger than the typical reconnection inflow speed 0.1  $V_A$ . As a result, magnetic flux is piled up in the reconnection inflow region and the magnetosphere is greatly compressed. The motion of Earth's magnetopause current sheet in the normal direction is also frequently observed by satellite, and the average speed is around 40 km/s (Paschmann et al., 2018; Phan & Paschmann, 1996). Based on the typical Alfven speed  $V_A = 200$ –500 km/s in the magnetosheath, the average motion speed of Earth's magnetopause current sheet is 0.08–0.2  $V_A$ , comparable to that in our experiment.

In Figure 5d, the average half width of the reconnection current sheet is around 9.5 cm during the first period. Based on the measured local electron density  $n_e \approx 2 \times 10^{13}$  cm<sup>-3</sup> using the Langmuir probes, the local ion and electron inertia lengths are  $d_i = 32.2$  cm and  $d_e = 0.12$  cm. Therefore, the half width of the reconnection current sheet is on the sub-ion scale,  $\delta \approx 0.3$   $d_i \approx 80$   $d_e$ . The sub-ion scale current sheet may be related to the broaden of the current sheet due to the magnetic island or some collision effects due to the short mean free path during this period. During the second period, the average half width is around 5.7 cm. Based on the local electron density  $n_e \approx 1 \times 10^{12}$  cm<sup>-3</sup>, the local ion and electron inertia lengths are  $d_i = 144.2$  cm and  $d_e = 0.53$  cm. Therefore, the half width of the reconnection current sheet is on the electron inertia scale,  $\delta \approx 11$   $d_e$ , comparable to MRX experiments which obtain  $\delta \approx 5.5$ –7.5  $d_e$  (Ren et al., 2008), indicating the formation of a current sheet mainly carried by electrons.

#### 4. Conclusions and Discussion

In this paper, we experimentally study magnetopause-like reconnection using SPERF. A magnetic geometry similar to Earth's magnetopause reconnection is firstly built in laboratory. During the experiment, we show the compression and rebound of the magnetosphere driven by the solar wind, and a reconnection current sheet is formed therein. During the first period, reconnection is asymmetric, and a bipolar Hall magnetic field is measured, the reconnection current sheet is long and multiple *x*-line reconnection develops with the formation of a magnetic

HUANG ET AL. 6 of 9

Acknowledgments

The SPERF, after 15 years of design and

construction, has officially opened to the

world for operation. We extend our

heartfelt thanks to all members of the

Program Advisory Committee for their

assistance in the design of this user facility.

This work was supported by the National

Key Research and Development Program

of China (2022YFA1604600).

island. During the second period, we observe a symmetric single x-line reconnection with quadrupole Hall magnetic field.

Laboratory study of asymmetric reconnection has been conducted in MRX, TREX, and OMEGA laser facility (Olson et al., 2016; Rosenberg et al., 2015; Yamada et al., 2018; Yoo et al., 2014, 2017), these experiments also apply to understand magnetopause reconnection. Compared with these works, the magnetic geometry and driving conditions are more similar to Earth's magnetopause in our experiment. We observe the compression and rebound of the magnetosphere, and the evolution of magnetic reconnection from an asymmetric, multiple x-line state to a symmetric, single x-line state for the first time. These results indicate that magnetopause reconnection is highly unsteady, where the degree of upstream asymmetry and the number of x-line can change rapidly. The degree of asymmetry between magnetosphere and magnetosheath can mediate the reconnection rate (Cassak & Shay, 2007; Liu et al., 2018) and energy conversion rate (Chang et al., 2023), which affect the global convection process. The change in the number of reconnection x-line is closely related to the formation and interaction of flux ropes, which greatly affect particle acceleration and energy transport processes at magnetopause. The formation of flux ropes through multiple x-line reconnection can also explain the flux transfer events typically observed at the magnetopause of Earth and other planets (Lee & Fu, 1985; Russell & Elphic, 1978; Slavin et al., 2010; Walker & Russell, 2012). This mechanism has been demonstrated by satellite observations and simulations (Chen et al., 2017; Guo et al., 2021; Hasegawa et al., 2010; Sun et al., 2019; Zhong et al., 2013). Our results further provide experimental evidence for this explanation.

In the current experiment, we use Argon plasma, the driving voltage in the coils and the ECR source power are also low. As a result, the spatial scale of the reconnection region normalized by ion inertia length is around  $1-3\ d_i$ , and the Lundquist number is around  $10^3$ . Both are too small compared with Earth's magnetopause. In the future, we will use Helium or Hydrogen plasma, and increase the driving voltage and the ECR power. Then we expect to have a reconnection region around  $10-20\ d_i$ , it is still too small compared with Earth, but comparable to Earth like planets such as Mercury. This will enable more comprehensive studies on three-dimensional, driven, magnetopause reconnection.

SPERF is a new platform opened to the world which is devoted to study fundamental physical processes in the magnetosphere. The results from SPERF can also support the upcoming joint CAS/ESA mission Solar Wind Magnetosphere Ionosphere Link Explorer (SMILE), which will study the interaction between the solar wind and Earth's magnetosphere via X-Ray and UV images of the magnetosphere and aurora (C. Wang & Branduardi-Raymond, 2018).

#### **Conflict of Interest**

The authors declare no conflicts of interest relevant to this study.

#### **Data Availability Statement**

The experiment data and scripts used to plot the figures are available at National Space Science Data Center, National Science and Technology Infrastructure of China via Huang (2025).

#### References

Angelopoulos, V., Artemyev, A., Phan, T. D., & Miyashita, Y. (2020). Near-Earth magnetotail reconnection powers space storms. *Nature Physics*, 16(3), 317–321. https://doi.org/10.1038/s41567-019-0749-4

Angelopoulos, V., McFadden, J. P., Larson, D., Carlson, C. W., Mende, S. B., Frey, H., et al. (2008). Tail reconnection triggering substorm onset. Science, 321(5891), 931–935. https://doi.org/10.1126/science.1160495

Burch, J. L., Torbert, R. B., Phan, T. D., Chen, L. J., Moore, T. E., Ergun, R. E., et al. (2016). Electron-scale measurements of magnetic reconnection in space. *Science*, 352(6290), aaf2939. https://doi.org/10.1126/science.aaf2939

Cassak, P. A., & Shay, M. A. (2007). Scaling of asymmetric magnetic reconnection: General theory and collisional simulations. *Physics of Plasmas*, 14(10), 102114. https://doi.org/10.1063/1.2795630

Chang, C., Huang, K., Lu, S., Wang, R., & Lu, Q. (2023). Energy conversion during asymmetric magnetic reconnection. *The Astrophysical Journal*, 943(2), 73. https://doi.org/10.3847/1538-4357/acaa3d

Chen, Y., Tóth, G., Cassak, P., Jia, X., Gombosi, T. I., Slavin, J. A., et al. (2017). Global three-dimensional simulation of Earth's dayside reconnection using a two-way coupled magnetohydrodynamics with embedded particle-In-cell model: Initial results. *Journal of Geophysical Research: Space Physics*, 122(10), 10318–10335. https://doi.org/10.1002/2017ja024186

Dai, L., Zhu, M., Ren, Y., Gonzalez, W., Wang, C., Sibeck, D., et al. (2024). Global-scale magnetosphere convection driven by dayside magnetic reconnection. *Nature Communications*, 15(1), 639. https://doi.org/10.1038/s41467-024-44992-y

HUANG ET AL. 7 of 9



#### **Geophysical Research Letters**

- 10.1029/2025GL117351
- DiBraccio, G. A., Slavin, J. A., Boardsen, S. A., Anderson, B. J., Korth, H., Zurbuchen, T. H., et al. (2013). MESSENGER observations of magnetopause structure and dynamics at Mercury. *Journal of Geophysical Research: Space Physics*, 118(3), 997–1008. https://doi.org/10. 1002/jgra 50123
- Dungey, J. W. (1961). Interplanetary magnetic field and the auroral zones. *Physical Review Letters*, 6(2), 47–48. https://doi.org/10.1103/PhysRevLett.6.47
- Eastwood, J. P., Phan, T. D., Øieroset, M., & Shay, M. A. (2010). Average properties of the magnetic reconnection ion diffusion region in the Earth's magnetotail: The 2001–2005 cluster observations and comparison with simulations. *Journal of Geophysical Research*, 115(A8), A08215. https://doi.org/10.1029/2009ja014962
- Egedal, J., Fasoli, A., & Nazemi, J. (2003). Dynamical plasma response during driven magnetic reconnection. *Physical Review Letters*, 90(13), 135003. https://doi.org/10.1103/PhysRevLett.90.135003
- Frey, H. U., Phan, T. D., Fuselier, S. A., & Mende, S. B. (2003). Continuous magnetic reconnection at Earth's magnetopause. *Nature*, 426(6966), 533–537. https://doi.org/10.1038/nature02084
- Greess, S., Egedal, J., Stanier, A., Daughton, W., Olson, J., Le, A., et al. (2021). Laboratory verification of electron-scale reconnection regions modulated by a three-dimensional instability. *Journal of Geophysical Research: Space Physics*, 126(7), e2021JA029316. https://doi.org/10.1029/2021ja029316
- Guo, J., Lu, S., Lu, Q., Lin, Y., Wang, X., Huang, K., et al. (2021). Structure and coalescence of magnetopause flux ropes and their dependence on IMF clock angle: Three-dimensional global hybrid simulations. *Journal of Geophysical Research: Space Physics*, 126(2), e2020JA028670. https://doi.org/10.1029/2020ia028670
- Hasegawa, H., Wang, J., Dunlop, M. W., Pu, Z. Y., Zhang, Q., Lavraud, B., et al. (2010). Evidence for a flux transfer event generated by multiple X-line reconnection at the magnetopause. *Geophysical Research Letters*, 37(16), L16101. https://doi.org/10.1029/2010g1044219
- Huang, K. (2025). Dataset for "Laboratory realization of magnetopause-like reconnection in Space Plasma Environment Research Facility (SPERF)" [Dataset]. V1, Science Data Bank. https://doi.org/10.57760/sciencedb.space.02835
- Huang, K., Ling, W., Tang, H., Guan, J., Ke, Y., & E, P. (2025). Two-dimensional particle-in-cell simulation of magnetic reconnection in Space Plasma Environment Research Facility (SPERF). *Physics of Plasmas*, 32(7), 072901. https://doi.org/10.1063/5.0271547
- Huddleston, D. E., Russell, C. T., Le, G., & Szabo, A. (1997). Magnetopause structure and the role of reconnection at the outer planets. *Journal of Geophysical Research*, 102(A11), 24289–24302. https://doi.org/10.1029/97ia02416
- Ji, H., & Daughton, W. (2011). Phase diagram for magnetic reconnection in heliophysical, astrophysical, and laboratory plasmas. *Physics of Plasmas*, 18(11), 111207. https://doi.org/10.1063/1.3647505
- Ji, H., Yoo, J., Fox, W., Yamada, M., Argall, M., Egedal, J., et al. (2023). Laboratory study of collisionless magnetic reconnection. Space Science Reviews, 219(8), 76. https://doi.org/10.1007/s11214-023-01024-3
- Ji, H., Yamada, M., Hsu, S., & Kulsrud, R. (1998). Experimental test of the Sweet-Parker model of magnetic reconnection. *Physical Review*
- Letters, 80(15), 3256–3259. https://doi.org/10.1103/PhysRevLett.80.3256

  Kumar, P., & Zhang, B. (2015). The physics of gamma-ray bursts & relativistic jets. Physics Reports, 561, 1–109. https://doi.org/10.1016/j.
- physrep.2014.09.008
  Lee, L. C., & Fu, Z. F. (1985). A theory of magnetic flux transfer at the Earth's magnetopause. *Geophysical Research Letters*, 12(2), 105–108.
- https://doi.org/10.1029/GL012i002p00105
  Ling, W., Jin, C.-G., Mao, A.-H., E, P., Wu, J., Zhu, G.-L., et al. (2022). Design and construction of the dipole magnet of the Space Plasma
- Eng, W., Jin, C.-G., Mao, A.-H., E, P., Wu, J., Zhu, G.-L., et al. (2022). Design and construction of the dipole magnet of the Space Plasma Environment Research Facility (SPERF) for simulating the Earth magnetosphere. *Vacuum*, 201, 111112. https://doi.org/10.1016/j.vacuum. 2022.111112
- Ling, W., Jing, C., Wan, J., Mao, A., Xiao, Q., Guan, J., et al. (2024). Design and construction of the near-earth space plasma simulation system of the Space Plasma Environment Research Facility. *Journal of Plasma Physics*, 90(1), 345900101. https://doi.org/10.1017/s0022377823001460
- Liu, Y. H., Hesse, M., Cassak, P. A., Shay, M. A., Wang, S., & Chen, L. J. (2018). On the collisionless asymmetric magnetic reconnection rate. Geophysical Research Letters, 45(8), 3311–3318. https://doi.org/10.1002/2017gl076460
- Lu, Q., Fu, H., Wang, R., & Lu, S. (2022). Collisionless magnetic reconnection in the magnetosphere. Chinese Physics B, 31(8), 089401. https://doi.org/10.1088/1674-1056/ac76ab
- Lyutikov, M., & Lazarian, A. (2013). Topics in microphysics of relativistic plasmas. Space Science Reviews, 178(2–4), 459–481. https://doi.org/10.1007/s11214-013-9989-2
- Masuda, S., Kosugi, T., Hara, H., & Ogawara, Y. (1994). A loop top hard X-Ray source in a compact solar-flare as evidence for magnetic reconnection. *Nature*, 371(6497), 495–497. https://doi.org/10.1038/371495a0
- McAndrews, H. J., Owen, C. J., Thomsen, M. F., Lavraud, B., Coates, A. J., Dougherty, M. K., & Young, D. T. (2008). Evidence for reconnection at Saturn's magnetopause. *Journal of Geophysical Research*, 113(A4), A04210. https://doi.org/10.1029/2007ja012581
- Mozer, F. S., Bale, S. D., & Phan, T. D. (2002). Evidence of diffusion regions at a subsolar magnetopause crossing. *Physical Review Letters*, 89(1), 015002. https://doi.org/10.1103/PhysRevLett.89.015002
- Øieroset, M., Phan, T. D., Eastwood, J. P., Fujimoto, M., Daughton, W., Shay, M. A., et al. (2011). Direct evidence for a three-dimensional magnetic flux rope flanked by two active magnetic ReconnectionXLines at Earth's magnetopause. *Physical Review Letters*, 107(16), 165007. https://doi.org/10.1103/PhysRevLett.107.165007
- Olson, J., Egedal, J., Greess, S., Myers, R., Clark, M., Endrizzi, D., et al. (2016). Experimental demonstration of the collisionless plasmoid instability below the ion kinetic scale during magnetic reconnection. *Physical Review Letters*, 116(25), 255001. https://doi.org/10.1103/PhysRevLett.116.255001
- Paschmann, G., Haaland, S. E., Phan, T. D., Sonnerup, B. U. Ö., Burch, J. L., Torbert, R. B., et al. (2018). Large-scale survey of the structure of the dayside magnetopause by MMS. *Journal of Geophysical Research: Space Physics*, 123(3), 2018–2033. https://doi.org/10.1002/2017ja025121
- Paschmann, G., Sonnerup, B. U. Ö., Papamastorakis, I., Sckopke, N., Haerendel, G., Bame, S. J., et al. (1979). Plasma acceleration at the Earth's magnetopause: Evidence for reconnection. *Nature*, 282(5736), 243–246. https://doi.org/10.1038/282243a0
- Phan, T. D., Kistler, L. M., Klecker, B., Haerendel, G., Paschmann, G., Sonnerup, B. U. Ö., et al. (2000). Extended magnetic reconnection at the Earth's magnetopause from detection of bi-directional jets. *Nature*, 404(6780), 848–850. https://doi.org/10.1038/35009050
- Phan, T. D., & Paschmann, G. (1996). Low-latitude dayside magnetopause and boundary layer for high magnetic shear: 1. Structure and motion. Journal of Geophysical Research, 101(A4), 7801–7815. https://doi.org/10.1029/95ja03752
- Pritchett, P. L. (2008). Collisionless magnetic reconnection in an asymmetric current sheet. *Journal of Geophysical Research*, 113(A6), A06210. https://doi.org/10.1029/2007ja012930
- Ren, Y., Yamada, M., Ji, H., Gerhardt, S. P., & Kulsrud, R. (2008). Identification of the electron-diffusion region during magnetic reconnection in a laboratory plasma. *Physical Review Letters*, 101(8), 085003. https://doi.org/10.1103/PhysRevLett.101.085003

HUANG ET AL. 8 of 9

- Rosenberg, M. J., Li, C. K., Fox, W., Igumenshchev, I., Séguin, F. H., Town, R. P. J., et al. (2015). A laboratory study of asymmetric magnetic reconnection in strongly driven plasmas. *Nature Communications*, 6(1), 6190. https://doi.org/10.1038/ncomms7190
- Russell, C. T., & Elphic, R. C. (1978). Initial ISEE magnetometer results: Magnetopause observations. Space Science Reviews, 22(6), 681–715. https://doi.org/10.1007/bf00212619
- Sang, L., Lu, Q., Xie, J., Fan, F., Zhang, Q., Ding, W., et al. (2022). Energy dissipation during magnetic reconnection in the Keda linear magnetized plasma device. *Physics of Plasmas*, 29(10), 102108. https://doi.org/10.1063/5.0090790
- Shay, M. A., Phan, T. D., Haggerty, C. C., Fujimoto, M., Drake, J. F., Malakit, K., et al. (2016). Kinetic signatures of the region surrounding the X line in asymmetric (magnetopause) reconnection. *Geophysical Research Letters*, 43(9), 4145–4154. https://doi.org/10.1002/2016g1069034
- Shi, P., Scime, E. E., Barbhuiya, M. H., Cassak, P. A., Adhikari, S., Swisdak, M., & Stawarz, J. E. (2023). Using direct laboratory measurements of electron temperature anisotropy to identify the heating mechanism in electron-only guide field magnetic reconnection. *Physical Review Letters*, 131(15), 155101. https://doi.org/10.1103/PhysRevLett.131.155101
- Shi, P., Srivastav, P., Barbhuiya, M. H., Cassak, P. A., Scime, E. E., & Swisdak, M. (2022). Laboratory observations of electron heating and non-Maxwellian distributions at the kinetic scale during electron-only magnetic reconnection. *Physical Review Letters*, 128(2), 025002. https://doi.org/10.1103/PhysRevLett.128.025002
- Shibata, K., Masuda, S., Shimojo, M., Hara, H., Yokoyama, T., Tsuneta, S., et al. (1995). Hot-plasma ejections associated with compact-loop solar-flares. *Astrophysical Journal*, 451(2), L83. https://doi.org/10.1086/309688
- Slavin, J. A., Acuña, M. H., Anderson, B. J., Baker, D. N., Benna, M., Boardsen, S. A., et al. (2009). MESSENGER observations of magnetic reconnection in Mercury's magnetosphere. Science, 324(5927), 606–610. https://doi.org/10.1126/science.1172011
- Slavin, J. A., Lepping, R. P., Wu, C., Anderson, B. J., Baker, D. N., Benna, M., et al. (2010). MESSENGER observations of large flux transfer events at Mercury. Geophysical Research Letters, 37(2), L02105. https://doi.org/10.1029/2009g1041485
- Sonnerup, B. U. Ö., Hasegawa, H., & Paschmann, G. (2004). Anatomy of a flux transfer event seen by cluster. *Geophysical Research Letters*, 31(11), L11803, https://doi.org/10.1029/2004gl020134
- Sonnerup, B. U. Ö., Smith, E. J., Tsurutani, B. T., & Wolfe, J. H. (1981). Structure of Jupiter's magnetopause: Pioneer 10 and 11 observations. Journal of Geophysical Research, 86(A5), 3321–3334. https://doi.org/10.1029/JA086iA05p03321
- Journal of Geophysical Research, 60(A3), 5321–5334. https://doi.org/10.1029/JA080IA03pU3321
  Stenzel, R. L., & Gekelman, W. (1981). Magnetic field line reconnection experiments 1. Field topologies. Journal of Geophysical Research, 86(A2), 649–658. https://doi.org/10.1029/JA086iA02p00649
- Sun, T. R., Tang, B. B., Wang, C., Guo, X. C., & Wang, Y. (2019). Large-scale characteristics of flux transfer events on the dayside magnetopause. Journal of Geophysical Research: Space Physics, 124(4), 2425–2434. https://doi.org/10.1029/2018ja026395
- Journal of Geophysical Research: Space Physics, 124(4), 2425–2434. https://doi.org/10.1029/2018ja026395

  Tanaka, K. G., Retinò, A., Asano, Y., Fujimoto, M., Shinohara, I., Vaivads, A., et al. (2008). Effects on magnetic reconnection of a density
- asymmetry across the current sheet. *Annales Geophysicae*, 26(8), 2471–2483. https://doi.org/10.5194/angeo-26-2471-2008
  Vaivads, A., Khotyaintsev, Y., André, M., Retinò, A., Buchert, S., Rogers, B., et al. (2004). Structure of the magnetic reconnection diffusion
- region from four-spacecraft observations. *Physical Review Letters*, 93(10), 105001. https://doi.org/10.1103/PhysRevLett.93.105001 Walker, R. J., & Russell, C. T. (2012). Flux transfer events at the Jovian magnetopause. *Journal of Geophysical Research*, 90(A8), 7397–7404.
- https://doi.org/10.1029/JA090iA08p07397
  Wang, C., & Branduardi-Raymond, G. (2018). Progress of solar wind magnetosphere ionosphere link explorer (SMILE) mission. *Chinese Journal*
- of Space Science, 38(5), 657. https://doi.org/10.11728/cjss2018.05.657

  Wang, R., Lu, Q., Nakamura, R., Baumjohann, W., Russell, C. T., Burch, J. L., et al. (2017). Interaction of magnetic flux ropes via magnetic reconnection observed at the magnetopause. Journal of Geophysical Research: Space Physics, 122(10), 10436–10447. https://doi.org/10.1002/
- Wang, R., Nakamura, R., Lu, Q., Baumjohann, W., Ergun, R. E., Burch, J. L., et al. (2017). Electron-scale quadrants of the hall magnetic field observed by the magnetospheric multiscale spacecraft during asymmetric reconnection. *Physical Review Letters*, 118(17), 175101. https://doi.
- Xie, J., Shi, P., Ji, H., Jara-Almonte, J., Yoo, J., Okunishi, Y., et al. (2024). Local dynamic responses of magnetic reconnection to three-dimensional perturbations in a laboratory plasma. *Physics of Plasmas*, 31(2), 022108. https://doi.org/10.1063/5.0187992
- Yamada, M., Chen, L. J., Yoo, J., Wang, S., Fox, W., Jara-Almonte, J., et al. (2018). The two-fluid dynamics and energetics of the asymmetric magnetic reconnection in laboratory and space plasmas. *Nature Communications*, 9(1), 5223. https://doi.org/10.1038/s41467-018-07680-2
- Yamada, M., Ji, H. T., Hsu, S., Carter, T., Kulsrud, R., Ono, Y., & Perkins, F. (1997). Identification of Y-shaped and O-shaped diffusion regions during magnetic reconnection in a laboratory plasma. *Physical Review Letters*, 78(16), 3117–3120. https://doi.org/10.1103/PhysRevLett.78.
- Yamada, M., Yoo, J., Jara-Almonte, J., Ji, H., Kulsrud, R. M., & Myers, C. E. (2014). Conversion of magnetic energy in the magnetic reconnection layer of a laboratory plasma. *Nature Communications*, 5(1), 4774. https://doi.org/10.1038/ncomms5774
- Yang, F., Lu, Q., Zhang, Q., Xie, J., Gao, X., Ke, Y., et al. (2025). Laboratory observations of hall magnetic field in electron-only magnetic reconnection with a guide field. Geophysical Research Letters, 52(7), e2024GL114151. https://doi.org/10.1029/2024g114151
- Yang, J., Xie, J., Ling, W., Guan, J., Huang, K., Chen, F., et al. (2024). Design of three-dimensional magnetic probe system for space plasma environment research facility (SPERF). Sensors, 24(16), 5302. https://doi.org/10.3390/s24165302
- Yoo, J., Na, B., Jara-Almonte, J., Yamada, M., Ji, H., Roytershteyn, V., et al. (2017). Electron heating and energy inventory during asymmetric reconnection in a laboratory plasma. *Journal of Geophysical Research: Space Physics*, 122(9), 9264–9281. https://doi.org/10.1002/2017ja024152
- Yoo, J., Yamada, M., Ji, H., Jara-Almonte, J., Myers, C. E., & Chen, L.-J. (2014). Laboratory study of magnetic reconnection with a density asymmetry across the current sheet. *Physical Review Letters*, 113(9), 095002. https://doi.org/10.1103/PhysRevLett.113.095002
- Zhong, J., Pu, Z. Y., Dunlop, M. W., Bogdanova, Y. V., Wang, X. G., Xiao, C. J., et al. (2013). Three-dimensional magnetic flux rope structure formed by multiple sequential X-line reconnection at the magnetopause. *Journal of Geophysical Research: Space Physics*, 118(5), 1904–1911. https://doi.org/10.1002/jgra.50281
- Zhou, M., Berchem, J., Walker, R., El-Alaoui, M., Deng, X., Cazzola, E., et al. (2017). Coalescence of macroscopic flux ropes at the subsolar magnetopause: Magnetospheric multiscale observations. *Physical Review Letters*, 119(5), 055101. https://doi.org/10.1103/PhysRevLett.119. 055101

HUANG ET AL. 9 of 9